Publishing House
AKAPIT

COMPUTER METHODS IN MATERIALS SCIENCE

Informatyka w Technologii Materiałów

Vol. 17, 2017, No. 1

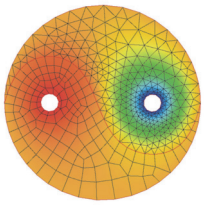

THE MLPG IN GRADIENT THEORY FOR SIZE-DEPENDENT MAGNETOELECTROELASTICITY

JAN SLADEK[1*], VLADIMIR SLADEK[1], SLAVOMIR HRCEK[2]

[1]Institute of Construction and Architecture, Slovak Academy of Sciences, 84503 Bratislava, Slovakia
[2]Faculty of Mechanical Engineering, University of Zilina, 01026 Zilina, Slovakia
**Corresponding author: sladek@savba.sk*

Abstract

The strain gradient magnetoelectroelasticity is applied to solve two-dimensional boundary value problems. The electric and magnetic field-strain gradient coupling is considered in constitutive equations. The meshless local Petrov-Galerkin (MLPG) is developed to solve general problems. All field quantities are approximated by the moving least-squares (MLS) scheme. Effective material properties for a piezomagnetic matrix with regularly distributed piezoelectric fibres of a circular cross section and coating layer are presented.

Key words: meshless approximation, local integral equations, MLS approximation, effective material properties

1. INTRODUCTION

It is well known that some composite materials can provide superior properties compared to their virgin monolithic constituent materials (Ryu et al., 2002). The spatial arrangement of the fibres and their geometry can influence the estimation of the effective material properties of the unidirectional composite. Magnetoelectroelastic (MEE) composites are made of piezoelectric and magnetostrictive phases coupled together. From earlier investigation for macro-sized layered MEE it is well-known that effective composite coefficients are higher than their constituent ones (Bishay et al., 2012). A similar enhancement of effective coefficients has been observed for fibered composites. Kuo and Wang (2012) optimized the effective magnetoelectric (ME) voltage coefficient of fibrous composites made of piezoelectric and piezomagnetic phases.

Due to the superior mechanical, electrical, optical, chemical and other properties, the nano/micro structures are utilized in many engineering fields. It is well known that nanostructures are size-dependent (Cross, 2006; Murmu & Pradhan, 2009; Ke et al., 2012; Liang et al., 2013). The size effect phenomenon is observed if the component dimension is comparable to the material length scale. The size dependent structures cannot be described by classical continuum mechanics due to the lack of the material length scale. Advanced continuum models with material length parameter are frequently applied for the investigation of nanomechanics due to their computational efficiency and the capability to give accurate results which are comparable to the atomistic models (Tang et al., 2005).

In the present paper, governing equations for magnetoelectroelastic solid in gradient elasticity with the corresponding boundary conditions are derived from the variational principle. In recent years, meshless formulations are becoming popular due to their high adaptability and low costs to prepare input and output data in numerical analysis.

ISSN 1641-8581

The moving least squares (MLS) approximation is generally considered as one of many schemes to interpolate discrete data with a reasonable accuracy. The meshless Petrov-Galerkin (MLPG) method (Sladek et al., 2013) is developed for the solution of boundary value problems in the gradient theory of magnetoelectroelasticity. The derived governing partial differential equations are satisfied in a weak form on small fictitious subdomains. Nodal points are introduced and spread on the analyzed domain and each node is surrounded by a small circle for simplicity, but without loss of shape generality. For a simple shape of subdomains like circles applied in this paper, numerical integrations over them can be easily carried out. The integral equations have a very simple nonsingular form. The spatial variations of the displacements, the electric and magnetic potentials are approximated by the MLS scheme (Atluri, 2004).

2. GOVERNING EQUATIONS FOR GRADIENT THEORY OF THE MEE

The electric field-strain gradient theory for nano-dielectrics has been introduced by Hu and Shen (2009). This theory is here extended for nano-magnetoelectrroelastic material. The constitutive equations for stresses, high-order stresses, electric displacement and magnetic induction are given by

$$\begin{aligned}
\sigma_{ij} &= c_{ijkl}\gamma_{kl} - e_{kij}E_k - q_{kij}H_k \\
\tau_{jkl} &= -f_{ijkl}E_i - h_{ijkl}H_i + g_{jklmni}\eta_{mni} \\
D_k &= e_{kij}\gamma_{ij} + \varepsilon_{kl}E_l + \alpha_{kl}H_l + f_{klmn}\eta_{lmn} \\
B_k &= q_{kij}\gamma_{ij} + \alpha_{kl}E_l + \mu_{kl}H_l + h_{klmn}\eta_{lmn}
\end{aligned} \tag{1}$$

where $\boldsymbol{\varepsilon}$, $\boldsymbol{\mu}$ and $\mathbf{c}$, are the second-order permittivity, permeability and the fourth-order elastic constant tensors, respectively. The symbol $\mathbf{e}$ denotes the piezoelectric coefficient, $\mathbf{q}$ is the piezomagnetic coefficient, $\boldsymbol{\alpha}$ is the electromagnetic coefficient, $\mathbf{f}$ is the electric field–strain gradient coupling coefficient tensor representing the higher-order electro-mechanical coupling induced by the strain gradient and $\mathbf{h}$ is the magnetic field–strain gradient coupling coefficient tensor. The tensor $\mathbf{g}$ represents the purely nonlocal elastic effects, i.e., the strain gradient elasticity.

The strain gradient tensor is defined as

$$\eta_{ijk} = \gamma_{ij,k} = \frac{1}{2}\left(u_{i,jk} + u_{j,ik}\right) \tag{2}$$

The higher-order elastic parameters g_{jklmni} are proportional to conventional elastic parameters c_{klmn} by the internal length material parameter l (Liang & Shen, 2013). Similarly the electric field-strain gradient and magnetic field-strain gradient coupling coefficient f_{ijkl} and h_{ijkl} is expressed by piezoelectric and piezomagnetic coefficients, respectively, and scaling parameter m.

Consider a piezoelectric solid in domain V with boundary Γ. The variation of electric Gibbs free energy in gradient theory of magnetoelectroelastic solids is given by

$$\delta U = \int_V \left(\sigma_{ij}\delta\varepsilon_{ij} + \tau_{ijk}\delta\eta_{ijk} + D_k\delta\phi_{,k} + H_k\delta\psi_{,k}\right)dV \tag{3}$$

Applying the Gauss divergence theorem one gets

$$\begin{aligned}
\delta U &= -\int_V \left(\sigma_{ij,j}\delta u_i + \tau_{ijk,k}\delta u_{i,j} + D_{k,k}\delta\phi + H_{k,k}\delta\psi\right)dV + \\
&+\int_\Gamma \left(n_j\sigma_{ij}\delta u_i + n_k\tau_{ijk}\delta u_{i,j} + n_k D_k\delta\phi + n_k H_k\delta\psi\right)d\Gamma = \\
&= -\int_V \left[\left(\sigma_{ij,j} - \tau_{ijk,jk}\right)\delta u_i + D_{k,k}\delta\phi + H_{k,k}\delta\psi\right]dV + \\
&\int_\Gamma \left\{t_i\delta u_i + R_i\delta s_i + Q\delta\phi + S\delta\psi\right\}d\Gamma
\end{aligned} \tag{4}$$

where π_i is the Cartesian component of the unit tangent vector on Γ, $s_i := \dfrac{\partial u_i}{\partial \mathbf{n}}$, $R_i := n_k n_j \tau_{ijk}$, $Q := n_k D_k$, $S := n_k H_k$ and the traction vector is defined as

$$t_i = n_j\left(\sigma_{ij} - \tau_{ijk,k}\right) - \frac{\partial \rho_i}{\partial \boldsymbol{\pi}} + \sum_c \left\|\rho_i(\mathbf{x}^c)\right\|\delta(\mathbf{x}-\mathbf{x}^c) \tag{5}$$

with $\rho_i := n_k\pi_j\tau_{ijk}$, and the jump at a corner on the oriented boundary contour Γ is defined as $\left\|\rho_i(\mathbf{x}^c)\right\| := \rho_i(\mathbf{x}^c + 0) - \rho_i(\mathbf{x}^c - 0)$.

The work of the external "forces" $\left(\overline{t}_i, \overline{R}_i, \overline{Q}, \overline{S}\right)$ is given by

$$\delta W = \int_{\Gamma_t} \overline{t}_i\delta u_i d\Gamma + \int_{\Gamma_R} \overline{R}_i\delta s_i d\Gamma + \int_{\Gamma_Q} \overline{Q}\delta\phi d\Gamma + \int_{\Gamma_S} \overline{S}\delta\psi d\Gamma \tag{6}$$

From the principle of virtual work $\delta U - \delta W = 0$, the following governing equations are obtained from

equations (4) and (6), since the variation $\delta u_i = 0$ on Γ_u

$$\sigma_{ij,j}(\mathbf{x}) - \tau_{ijk,jk}(\mathbf{x}) = 0$$
$$D_{k,k}(\mathbf{x}) = 0 \qquad (7)$$
$$H_{k,k}(\mathbf{x}) = 0$$

3. THE MESHLESS PETROV GALERKIN METHOD

According to the meshless local Petrov-Galerkin (MLPG) method, we construct a weak-form of (1) over the local subdomains Ω_s around each node $\mathbf{x}^{\mathrm{i}}$ inside the global domain V (Sladek et al., 2013). The local weak-form of the first governing equation (7) can be written as

$$\int_{\Omega_s} \left[\sigma_{ij,j}(\mathbf{x}) - \tau_{ijk,jk}(\mathbf{x})\right] u^*_{ik}(\mathbf{x})\, d\Omega = 0 \qquad (8)$$

where $u^*_{ik}(\mathbf{x})$ is a test function. The test function can be arbitrary.

By choosing a Heaviside step function as the test function $u^*_{ik}(\mathbf{x})$ in each subdomain as

$$u^*_{ik}(\mathbf{x}) = \begin{cases} \delta_{ik} & \text{at} \quad \mathbf{x} \in \Omega_s \\ 0 & \text{at} \quad \mathbf{x} \notin \Omega_s \end{cases},$$

the local weak-form (8) is converted into the following local boundary integral equations

$$\int_{L_s+\Gamma_{su}} n_j \left(\sigma_{ij} - \tau_{ijk,k}\right) d\Gamma + \rho_i(\mathbf{x}^f_{st}) - \rho_i(\mathbf{x}^s_{st}) = -\int_{\Gamma_{st}} \overline{t}_i d\Gamma \qquad (9)$$

where definition of the traction vector (5) is utilized and $\mathbf{x}^f_{st}$, $\mathbf{x}^s_{st}$ stand for the final and starting points on Γ_{st}. Here, L_s is the local boundary that is totally inside the global domain, Γ_{st} is the part of the local boundary which coincides with the global traction boundary, and similarly Γ_{su} is the part of the local boundary that coincides with the global displacement boundary.

Similarly, the local boundary integral equations are derived for the second and third governing equation (7)

$$\int_{L_s+\Gamma_{s\phi}} Q(\mathbf{x}) d\Gamma = -\int_{\Gamma_{sQ}} \overline{Q}(\mathbf{x}) d\Gamma \qquad (10)$$

$$\int_{L_s+\Gamma_{s\psi}} S(\mathbf{x}) d\Gamma = -\int_{\Gamma_{sS}} \overline{S}(\mathbf{x}) d\Gamma \qquad (11)$$

where

$$Q(\mathbf{x}) = D_k(\mathbf{x}) n_k(\mathbf{x}) =$$
$$\left[e_{kij} u_{i,j}(\mathbf{x}) - \varepsilon_{kl}\phi_{,l}(\mathbf{x}) - \alpha_{kl}\psi_{,l}(\mathbf{x}) + f_{klmn} u_{l,mn}(\mathbf{x})\right] n_k$$

$$S(\mathbf{x}) = B_k(\mathbf{x}) n_k(\mathbf{x}) =$$
$$\left[q_{kij} u_{i,j}(\mathbf{x}) - \alpha_{kl}\phi_{,l}(\mathbf{x}) - \mu_{kl}\psi_{,l}(\mathbf{x}) + h_{klmn} u_{l,mn}(\mathbf{x})\right] n_j$$

In the present paper the trial functions are approximated by the moving least squares (MLS) method on a number of nodes spread over the influence domain (Sladek et al., 2013). One can write

$$\mathbf{u}^h(\mathbf{x}) = \mathbf{N}^T(\mathbf{x}) \cdot \hat{\mathbf{u}} = \sum_{a=1}^{n} N^a(\mathbf{x}) \hat{\mathbf{u}}^a$$
$$\phi^h(\mathbf{x}) = \sum_{a=1}^{n} N^a(\mathbf{x}) \hat{\phi}^a \qquad (12)$$
$$\psi^h(\mathbf{x}) = \sum_{a=1}^{n} N^a(\mathbf{x}) \hat{\psi}^a$$

where the nodal values $\hat{\mathbf{u}}^a = \left(\hat{u}^a_1, \hat{u}^a_3\right)^T$, $\hat{\phi}^a$ and $\hat{\psi}^a$ are fictitious parameters for the displacements, the electric and magnetic potentials, respectively, and $N^a(\mathbf{x})$ is the shape function associated with the node a. The number of nodes n used for the approximation is determined by the weight function $w^a(\mathbf{x})$. A 4th order spline-type weight function is applied in the present work.

The traction vectors $t_i(\mathbf{x})$, electric charge $Q(\mathbf{x})$ and magnetic flux $S(\mathbf{x})$ at a boundary point $\mathbf{x} \in \partial\Omega_s$ can be approximated in terms of primary fields. Substituting these expressions into the local integral equations (9)-(11) one obtains a system of ordinary differential equations for nodal quantities

$$\sum_{a=1}^{n} \left(\int_{L_s+\Gamma_{st}} \mathcal{N}(\mathbf{x}) \mathbf{C} \mathbf{B}^a(\mathbf{x}) d\Gamma + \right.$$
$$\left. \int_{L_s+\Gamma_{st}} l^2 \mathcal{N}(\mathbf{x}) \mathbf{C} \left(\mathbf{B}^a_1(\mathbf{x}) + \mathbf{B}^a_3(\mathbf{x})\right) d\Gamma \right) \hat{\mathbf{u}}^a +$$
$$+ \sum_{a=1}^{n} \left(\int_{L_s+\Gamma_{sQ}} \mathcal{N}(\mathbf{x}) \mathbf{L} \mathbf{P}^a(\mathbf{x}) d\Gamma - \right.$$

$$\int_{L_s+\Gamma_{sQ}} m^2 \mathcal{N}(\mathbf{x})\mathbf{L}\left(\mathbf{P}_1^a(\mathbf{x})+\mathbf{P}_3^a(\mathbf{x})\right)d\Gamma\Bigg)\hat{\phi}^a \; +$$

$$+\sum_{a=1}^{n}\Bigg(\int_{L_s+\Gamma_{sS}} \mathcal{N}(\mathbf{x})\mathbf{M}\mathbf{P}^a(\mathbf{x})d\Gamma -$$

$$\int_{L_s+\Gamma_{sS}} \mathcal{N}(\mathbf{x})\mathbf{M}\left(\mathbf{P}_1^a(\mathbf{x})+\mathbf{P}_3^a(\mathbf{x})\right)d\Gamma\Bigg)\hat{\psi}^a \; +$$

$$+l^2\left\{\mathbf{\Pi}(\mathbf{x}_{st}^f)\mathbf{C}\left[\mathbf{B}_1^a(\mathbf{x}_{st}^f)+\mathbf{B}_3^a(\mathbf{x}_{st}^f)\right]-\right.$$

$$\left.-\mathbf{\Pi}(\mathbf{x}_{st}^s)\mathbf{C}\left[\mathbf{B}_1^a(\mathbf{x}_{st}^s)+\mathbf{B}_3^a(\mathbf{x}_{st}^s)\right]\right\}\hat{\mathbf{u}}^a = -\int_{\Gamma_{st}} \bar{\mathbf{t}}(\mathbf{x})d\Gamma \qquad (13)$$

$$\sum_{a=1}^{n}\Bigg(\int_{L_s+\Gamma_{sQ}} \mathbf{N}_1(\mathbf{x})\mathbf{L}^T\mathbf{B}^a(\mathbf{x})d\Gamma - \int_{L_s+\Gamma_{sQ}} m^2\mathbf{N}_1(\mathbf{x})\mathbf{L}^T\mathbf{B}_1^a(\mathbf{x})d\Gamma -$$

$$\int_{L_s+\Gamma_{sQ}} m^2\mathbf{N}_1(\mathbf{x})\mathbf{L}^T\mathbf{B}_3^a(\mathbf{x})d\Gamma\Bigg)\hat{\mathbf{u}}^a \; -$$

$$-\sum_{a=1}^{n}\Bigg(\int_{L_s+\Gamma_{sQ}} \mathbf{N}_1(\mathbf{x})\mathbf{J}\mathbf{P}^a(\mathbf{x})d\Gamma\Bigg)\hat{\phi}^a -$$

$$\sum_{a=1}^{n}\Bigg(\int_{L_s+\Gamma_{sS}} \mathbf{N}_1(\mathbf{x})\mathbf{A}\mathbf{P}^a(\mathbf{x})d\Gamma\Bigg)\hat{\psi}^a = -\int_{\Gamma_{sQ}} \bar{Q}(\mathbf{x})d\Gamma \qquad (14)$$

$$\sum_{a=1}^{n}\Bigg(\int_{L_s+\Gamma_{sS}} \mathbf{N}_1(\mathbf{x})\mathbf{M}^T\mathbf{B}^a(\mathbf{x})d\Gamma + \int_{L_s+\Gamma_{sS}} \mathbf{N}_1(\mathbf{x})\mathbf{M}^T\mathbf{B}_1^a(\mathbf{x})d\Gamma +$$

$$\int_{L_s+\Gamma_{sS}} \mathbf{N}_1(\mathbf{x})\mathbf{M}^T\mathbf{B}_3^a(\mathbf{x})d\Gamma\Bigg)\hat{\mathbf{u}}^a \; -$$

$$-\sum_{a=1}^{n}\Bigg(\int_{L_s+\Gamma_{sQ}} \mathbf{N}_1(\mathbf{x})\mathbf{A}\mathbf{P}^a(\mathbf{x})d\Gamma\Bigg)\hat{\phi}^a -$$

$$\sum_{a=1}^{n}\Bigg(\int_{L_s+\Gamma_{sS}} \mathbf{N}_1(\mathbf{x})\mathbf{I}\mathbf{P}^a(\mathbf{x})d\Gamma\Bigg)\hat{\psi}^a = -\int_{\Gamma_{sS}} \bar{S}(\mathbf{x})d\Gamma \qquad (15)$$

where

$$\mathcal{N}(\mathbf{x}) = \begin{bmatrix} n_1 & 0 & n_3 \\ 0 & n_3 & n_1 \end{bmatrix}, \quad \mathbf{N}_1(\mathbf{x}) = \begin{bmatrix} n_1 & n_3 \end{bmatrix},$$

$$\mathbf{\Pi}(\mathbf{x}) = \begin{bmatrix} \pi_1 & 0 & \pi_3 \\ 0 & \pi_3 & \pi_1 \end{bmatrix}$$

$$\mathbf{B}^a(\mathbf{x}) = \begin{bmatrix} N^a_{,1} & 0 \\ 0 & N^a_{,3} \\ N^a_{,3} & N^a_{,1} \end{bmatrix}, \quad \mathbf{B}_1^a(\mathbf{x}) = \begin{bmatrix} N^a_{,11} & 0 \\ 0 & N^a_{,31} \\ N^a_{,31} & N^a_{,11} \end{bmatrix},$$

$$\mathbf{B}_3^a(\mathbf{x}) = \begin{bmatrix} N^a_{,13} & 0 \\ 0 & N^a_{,33} \\ N^a_{,33} & N^a_{,13} \end{bmatrix},$$

$$\mathbf{P}^a(\mathbf{x}) = \begin{bmatrix} N^a_{,1} \\ N^a_{,3} \end{bmatrix}, \quad \mathbf{P}_1^a(\mathbf{x}) = \begin{bmatrix} N^a_{,11} \\ N^a_{,31} \end{bmatrix},$$

$$\mathbf{P}_3^a(\mathbf{x}) = \begin{bmatrix} N^a_{,13} \\ N^a_{,33} \end{bmatrix}.$$

The matrices $\mathbf{C}$, $\mathbf{L}$, and $\mathbf{M}$ represent material coefficients in the constitutive equation (1) for stresses. Similarly, the matrices $\mathbf{L}^{\mathbf{T}}$, $\mathbf{J}$, and $\mathbf{A}$ correspond to electrical displacements.

4. COATED CIRCULAR PIEZOELECTRIC FIBER IN PIEZOMAGNETIC MATRIX

The proposed computational method is applied for evaluation of effective material parameters for a piezomagnetic matrix with regularly distributed piezoelectric fibres of a circular cross section. For a regular distribution of fibres it is sufficient to consider only one fibre in the square domain ($a \times a$) as the RVE (figure 1). The polarization in our numerical analyses is considered in transversal direction, x_3-axis.

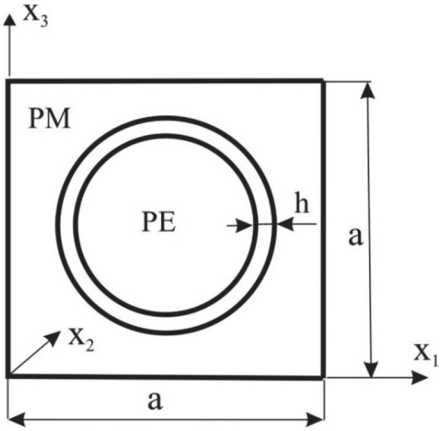

Fig. 1. Representative volume element (RVE) with piezomagnetic phase as matrix and piezoelectric phase as embedded fibre which has a coating layer of thickness h.

The effective material coefficients of MEE solids are computed from the constitutive equations rewritten for the average values of the secondary fields and the average values of conjugated fields

$$\langle \sigma_{ij} \rangle = \frac{1}{a^2} \int_{\Omega} \sigma_{ij} d\Omega; \quad \langle D_i \rangle = \frac{1}{a^2} \int_{\Omega} D_i d\Omega;$$

$$\langle B_i \rangle = \frac{1}{a^2} \int_{\Omega} B_i d\Omega \tag{16}$$

If a uniform strain along x_1 and vanishing electric and magnetic potentials are considered as we get following average values of the secondary fields

$$\langle \gamma_{11} \rangle = \overline{\gamma}_{11} = const\,, \ \langle \gamma_{33} \rangle = 0\,, \ \langle \gamma_{13} \rangle = 0\,, \ \langle E_i \rangle = 0\,,$$
$$\langle H_i \rangle = 0\,, \ \langle \eta_{ijk} \rangle = 0\,.$$

By this way we are able to compute following effective material parameters c_{11}^{eff}, c_{13}^{eff}, e_{31}^{eff}, q_{31}^{eff}. Similarly, we consider a uniform strain along x_3 and vanishing electric and magnetic potentials and analogically uniform electric intensity and magnetic fields are considered in several boundary value problems.

In numerical analyses the fibre is coated by the piezomagnetic material Terfenol-D. The matrix material parameter is $CoFe_2O_4$ and values are given in work (Pan & Chen, 2015). The piezoelectric fibre is consider as $BaTiO_3$.

The strain-gradient piezoelectric model can be reduced to the classical piezoelectric model if the internal length material parameter, l, and scaling parameter, m, appearing in constitutive equations vanish. The classical piezoelectric model has been analyzed in earlier author`s paper (Sladek et al., 2016a). In order to assess the size effect, we can introduce the strain-gradient size-factor, q, as

$$l^2 = q \cdot l_0^2, \ m^2 = q \cdot m_0^2$$

where $m_0^2 = 2\times10^{-8}\,\mathrm{m}$ and $l_0 = 5\times10^{-9}\,\mathrm{m}$ are fixed parameters selected for PZT5-H (Sladek et al. 2016b), where microstructure is similar to Terfenol-D. A very fine regular node distribution with 18988 nodes has been employed.

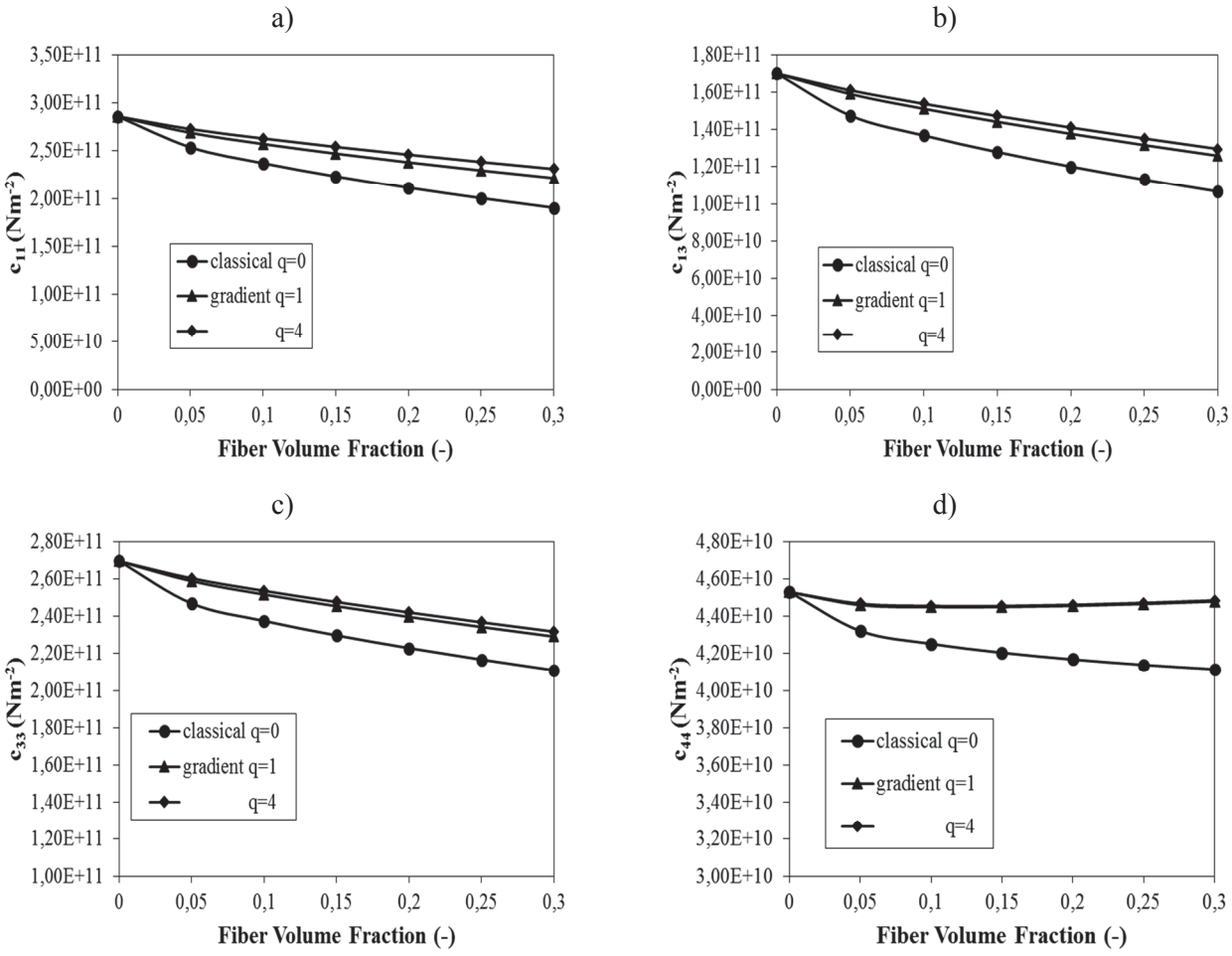

Fig. 2. *Variation of effective elastic coefficients with volume fraction of coated fibre*

Effective material parameters are computed for the values of fibre volume fraction in interval from 0.05 to 0.3. The numerical results for effective elastic material parameters are presented in figure 2. All effective elastic coefficients decrease with growing fibre volume fraction. One can also observe that effective elastic coefficients increase with increasing strain gradient parameter q, but are saturated when q equals 4. However, this enhancement is not significant due to a small volume fraction of the cladding layer on the whole composite content.

Variation of effective magnetoelectric coefficients with volume fraction of coated fibre is shown in figure 3. The magnitude of these coefficients increases if the volume fraction is increasing. One can also observe a strong influence of strain gradient theory on the effective magnetoelectric coefficients. The effective magnetoelectric coefficients are enhanced as compared to classical model, particularly when q is large.

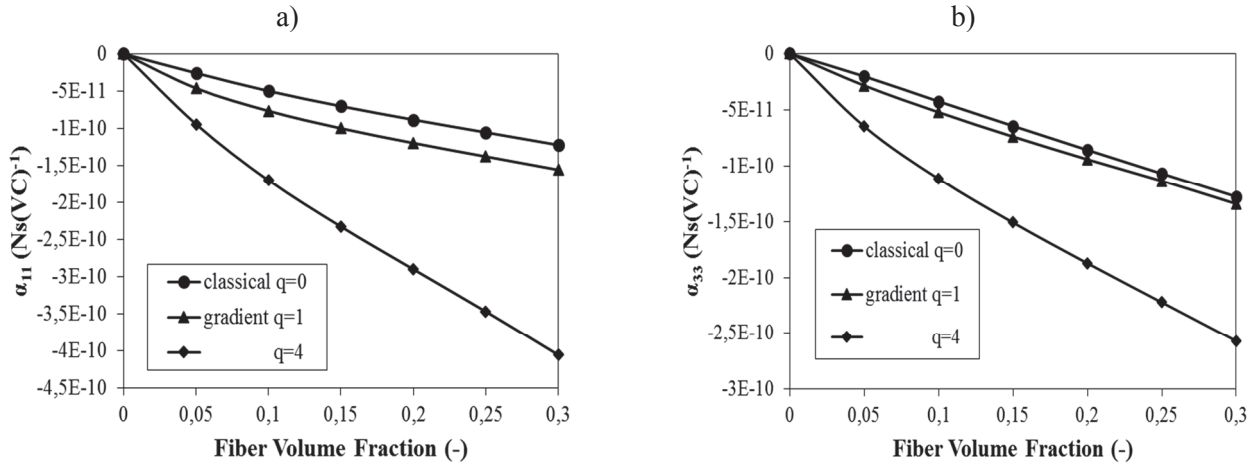

Fig. 3. *Variation of effective magnetoelectric coefficients with volume fraction of coated fibre*

5. CONCLUSIONS

The MLPG method is developed for the evaluation of effective material properties in MEE composite materials described by a gradient theory. The electric and magnetic field-strain gradient coupling is considered in constitutive equations. The governing equations are derived by virtue of the variational principle. The local integral equations for the solution of 2D boundary value problems of magnetoelectroelasticity are derived too.

It follows from numerical analyses that effective elastic and magnetoelectric (ME) coefficients are influenced significantly by strain-gradients. A stronger influence of the coating layer is observed for the effective magnetoelectric coefficient. The influence of the coating layer on the effective ME coefficient is dominant although the ME coefficients for all three composite constituents (fibre, matrix, coating) are zero.

The strain-gradient theory should be employed if the the dimensions of the analyzed problem are of the same order of magnitude as the internal material length. Numerical results illustrate that size-effect phenomenon has to be considered in such cases.

ACKNOWLEDGEMENT

The authors gratefully acknowledge the supports by the Slovak Science and Technology Assistance Agency registered under number APVV-14-216 and VEGA 1/0145/17.

REFERENCES

Atluri, S.N., 2004, *The Meshless Method (MLPG) for Domain and BIE Discretizations*, Tech Science Press, Forsyth.

Bishay, P.L., Sladek, J., Sladek, V., Atluri, S.N. 2012, Analysis of functionally graded multiferroic composites using hybrid/mixed finite elements and node-wise material properties, *CMC: Computers, Materials & Continua*, 29, 213-262.

Cross, L.E. 2006, Flexoelectric effects: charge separation in insulating solids subjected to elastic strain gradients, *J. Mater. Sci*., 41, 53-63.

Hu, S.L., Shen, S.P. 2009, Electric field gradient theory with surface effect for nano-dielectrics, *CMC: Computers, Materials & Continua*, 13, 63-87.

Ke, L. L., Wang, Y.S., Wang, Z.D. 2012, Nonlinear vibration of the piezoelectric nanobeams based on the nonlocal theory, *Comp. Struct.,* 94, 2038-2047.

Kuo, H.Y., Wang, Y.L. 2012, Optimization of magnetoelectricity in multiferroic fibrous composites. *Mechanics of Materials*, 50, 88-99.

Liang, X., Shen, S.P. 2013, Size-dependent piezoelectricity and elasticity due to the electric field-strain gradient coupling and strain gradient elasticity, *Int. J. Appl. Mech*., 5, 1350015.

Liang, X., Hu, S., Shen, S. 2013, Bernoulli-Euler dielectric beam model based on strain-gradient effect, *J. Appl. Mech.,* 80, 044502-6.

Murmu, T., Pradhan, S.C. 2009, Thermo-mechanical vibration of a single-walled carbon nanotube embedded in an elastic medium based on nonlocal elasticity theory, *Comput. Mater. Sci.*, 46, 854-859.

Pan, E., Chen, W. 2015, *Static Green's Functions in Anisotropic Media*, Cambridge University Press, New York.

Ryu, J., Priya, S., Uchino, K., Kim, H.E. 2002, Magnetoelectric effect in composites of magnetostrictive and piezoelectric materials, *Jour. Electroceramics*, 8, 107-119.

Sladek, J., Stanak, P., Han, Z.D., Sladek, V. Atluri, S.N., 2013, Applications of the MLPG method in engineering & sciences: A review, *CMES-Computer Model. Engn. Sci*., 92, 423-475.

Sladek, J., Sladek, V., Pan, E. 2016a, Effective properties of coated fiber-composites with piezoelectric and piezomagnetic phases. *Jour. Intell. Mater. Syst. Struct.,* DOI: 10.1177/1045389X16644786.

Sladek, J., Sladek, V., Pan, E. 2016b, Effective properties of coated fiber-composites with piezoelectric and piezomagnetic phases. *Int. J. Solids Struct.* DOI: 10.1016/j.ijsolstr.2016.08.011 .

Tang, Z., Xu, Y., Li, G., Aluru, N.R. 2005, Physical models for coupled electromechanical analysis of silicon nanoelectromechanical systems, *J. Appl. Phys*., 97, 114304.

BEZSIATKOWA LOKALNA METODA PETROVA-GALERKINA W GRADIENTOWEJ TEORII DLA ZALEŻNYCH OD ROZMIARU PROBLEMÓW W MAGNETOELEKTROSPRĘŻYSTOŚCI

Streszczenie

Celem pracy było zastosowanie magneto-elektro-sprężystości charakteryzującej się gradientem odkształceń do rozwiązania problemu brzegowego w domenie 2D. Prawo konstytutywne stanowi problem pól elektrycznego i magnetycznego sprzężonych z odkształceniami. Do rozwiązania ogólnego zadania wykorzystano bezsiatkową lokalną metodę Petrova-Galerkina (ang. the meshless local Petrov-Galerkin - MLPG). Wszystkie równania pola przybliżono metodą ruchomych najmniejszych kwadratów (ang. the moving least-squares - MLS). Wyznaczono efektywne własności materiałowe dla piezomagnetycznej osnowy z równomiernie rozłożonymi piezoelektrycznymi włóknami o okrągłym przekroju poprzecznym i pokrytych warstwą.

Received: November 7, 2016
Received in a revised form: December 18, 2016
Accepted: December 23, 2016